catalysts

MDPI

Article

Isomerization of Hemicellulose Aldoses to Ketoses Catalyzed by Basic Anion Resins: Catalyst Screening and Stability Studies

Miriam El Tawil-Lucas, Maia Montaña *, Miguel Macias-Villasevil, Jovita Moreno and Jose Iglesias *

Chemical & Environmental Engineering Group, Universidad Rey Juan Carlos, C/Tulipán, s/n, Mostoles, 28933 Madrid, Spain

* Correspondence: maia.montana@urjc.es (M.M.); jose.iglesias@urjc.es (J.I.)

Abstract: Isomerization of aldoses to ketoses is an essential step in carbohydrate valorization routes in biorefineries to produce a wide variety of bioproducts. In this work, selective isomerization of aldoses into ketoses was investigated using different commercial Brønsted basic anion resins at low temperature conditions. Weak and strong basic resins were tested under different reaction conditions. Amberlite IRA-900 and Amberlyst A-26 (strong resins) and Amberlite IRA-67 and Amberlyst A-21 (weak resins) were tested to assess their catalytic properties. Strong basic resins provided high yields of fructose. IRA-900 was also tested in the isomerization of different sugar monosaccharides conventionally present in lignocellulosic biomass (xylose, arabinose, galactose, glucose and mannose) aiming to explore the performance of this material in hemicellulose-derived sugar mixtures. Very promising performance was observed for IRA-900, yielding fructose selectivity higher than 75% and fructose yield of 27% in the isomerization reaction. Notably, basic anionic resins were not suitable for reuse in different reaction cycles, although the use of organic cosolvents, specifically ethanol, improved the reusability of the tested resins.

Keywords: isomerization; glucose; fructose; basic anion resins; hemicellulose

Citation: El Tawil-Lucas, M.; Montaña, M.; Macias-Villasevil, M.; Moreno, J.; Iglesias, J. Isomerization of Hemicellulose Aldoses to Ketoses Catalyzed by Basic Anion Resins: Catalyst Screening and Stability Studies. *Catalysts* **2023**, *13*, 1301. https://doi.org/10.3390/catal13091301

Academic Editor: Yi Wei

Received: 31 July 2023
Revised: 31 August 2023
Accepted: 11 September 2023
Published: 16 September 2023

1. Introduction

Lignocellulosic biomass is one of the most abundant renewable carbon sources for chemical manufacture, showing a high potential to substitute fossil resources in the preparation of chemicals. Lignocellulosic biomass is composed of three fractions: cellulose (40–50%), hemicellulose (25–30%) and lignin (15–20%), whose composition vary as a function of the starting feedstock [1–4]. Even though the valorization of these three factions has received the attention of scientists throughout several pathways [5], hemicellulose-derived sugars have been less explored as biorefinery raw materials, most likely because their composition makes a chemical valorization quite difficult. Hemicelluloses are composed of heterogeneous polymers of pentoses (xylose and arabinose), hexoses (glucose, mannose, and galactose), and some sugar acids (glucuronic acid and galacturonic acid) [6]. Beyond the production of furfural, which is a mature technology [7], most sugars in hemicellulose hydrolysates are usually discarded. However, profitable biorefinery schemes require the integral valorization of the starting biomass, including the hemicellulose fraction as crucial to reach an economically sustainable biorefinery process. In this context, the isomerization of hemicellulose-derived sugars (to transform aldoses into ketoses) is an industrially relevant process, as it is the first step in producing highly versatile furanics such as furfural or 5-hydroxymethylfurfural (5-HMF), two of the most relevant biomass-derived platform chemicals; thus, the evaluation of this pathway in the valorization of hemicellulose sugars is the most interesting.

The isomerization of aldoses to ketoses has been extensively explored through enzymatic and chemocatalytic routes. Enzymatic isomerization of monosaccharides has been reported since the mid-20th century, using different isomerase families and conducting

well-established industrial production process, as their efficiency is much higher than any other route [8]. Nevertheless, and in spite of the very high productivity [9,10] and the implantation of large-scale industrial processes [11], enzymatic isomerization still has important drawbacks, such as low enzyme stability, very limited operational conditions, and high operation expenditures. Chemocatalytic transformations, on the other hand, have been less explored, and they usually provide poorer results as compared to enzymatic processes; however, they have the advantage of being conducted under a wider range of operational conditions, and there is still quite a margin for improvement, so that these are considered a future promising alternative to enzymatic isomerization. Chemocatalytic isomerization of sugars can be conducted either in the presence of (Lewis) acid [12–15] or alkali catalysts [16]. Mechanisms with these two types of catalysts slightly differ (Scheme 1), since Lewis acid catalysts have been reported to act by binding the aldose to the catalytic sites, in a bidentate manner, through the aldehyde and the adjacent hydroxyl group, and promoting an internal molecular hydrogen shift, which finally conducts to the ketose [17]. On the other hand, basic catalysts promote a proton transfer mechanism, conventionally known as the Lobry de Bruyn–Alberda van Ekenstein mechanism [18,19], in which the deprotonation of the α-carbon of the aldose occurs, providing an enolate intermediate, which undergoes a hydrogen transfer to produce the ketose [20,21].

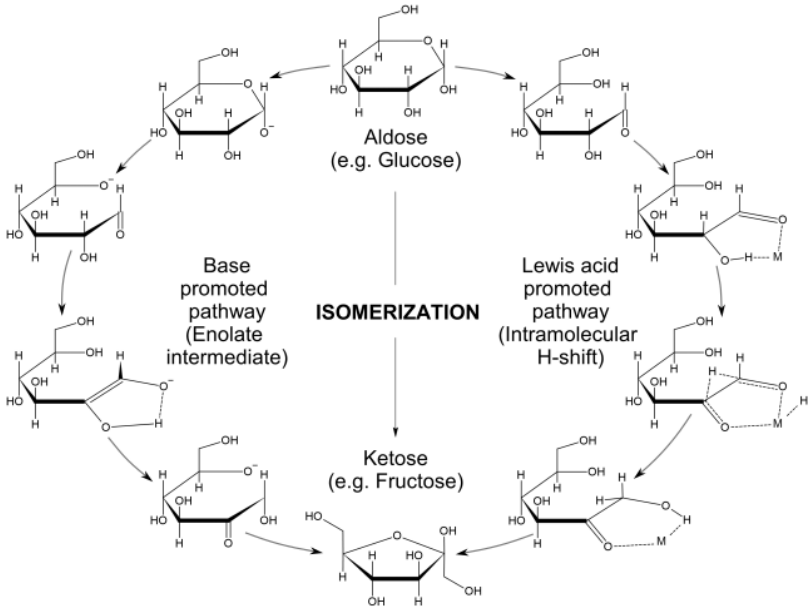

Scheme 1. Mechanisms of Base/Lewis acid catalytic isomerization of aldoses to ketoses.

As for the catalytic systems reported in the literature, remarkable fructose yields have been reported by using USY [22] and Sn-β zeolites [16,23] operating in different reaction media (water and methanol as solvents). However, these catalysts, bearing highly active Lewis acid sites, do not lack drawbacks and they have been described as suffering several deactivation phenomena [15]; thus, these processes are difficult to be scale up to industrial production. On the other hand, the chemical isomerization of sugars with alkalis has been reported in a higher extension. It was first explored in the presence of homogeneous base catalysts (NaOH, KOH), but their low catalytic performance (ketose yields < 15%) and poor carbon balances [24] soon conducted to explore different catalytic systems. The addition catalyst additives, like borates [25] and aluminates [26], was a major scientific breakthrough in the study of chemical isomerization of sugars, providing fructose yields from glucose above 70%. However, this pathway is highly complex and achieving its leap to an industrial scale may be difficult. Regarding heterogeneous base catalysts, most successful examples include Mg- and Ca-containing hydrotalcites, Mg- or Ca-functionalized zeolites and different oxide mixtures (CaO-MgO, CaO-Al_2O_3, CaO-ZrO_2, MgO-ZrO_2, etc.) [18,27]. Likewise, anion exchange resins (AERs) have also been

reported as efficient catalysts for the isomerization of glucose into fructose [28]. The main advantages of AERs are the high availability in high quantities to be applied at an industrial scale. In addition, these materials have been described to be excellent catalysts for sugar isomerization, although the type of resin is one of the most relevant factors conditioning the activity and selectivity of the transformation [29].

Isomerization of other sugars, different from glucose, such as xylose, arabinose, galactose, and mannose, can produce value-added products, but these substrates have been poorly exploited [30,31]. Aiming to fill this gap and looking for an integral biomass valorization that will include a whole use of the hemicellulose fraction, the present work explores the versatility of four commercial AERs for the selective isomerization of different sugars (xylose, arabinose, glucose, galactose, and mannose). The effect of different variables, such as the reaction temperature, the type of active sites or the addition of cosolvents to prevent catalyst deactivation, have all been thoroughly evaluated. Additionally, a mixture of aldoses mocking sugar hemicellulose hydrolysates have also been valorized. The use of these complex mixtures of sugars aims at testing the versatility and the applicability of the base-catalyzed isomerization process as valorization routes for these cheap and plenty raw materials liable to be used in future biorefineries.

2. Results and Discussion

Commercially available macroreticular and gel-type resins were tested to compare their activity as Brønsted-type basic catalysts for the isomerization of aldoses into ketoses. For this purpose, Amberlyst A-21, Amberlyst A-26, AmberLite IRA-67, and AmberLite IRA-900 resins, combining strong and weak basic sites, were selected. A-21, A-26 and IRA-900 materials are macroreticular resins formed of styrene-divinylbenzene copolymer matrices bearing tertiary amine (weak) and quaternary ammonium (strong) Brønsted-type basic groups as terminal functionalities. IRA-67 is a gel-type resin formed of crosslinked acrylic copolymer. Table 1 lists the main physicochemical properties of these materials.

Table 1. Physicochemical properties of tested anion exchange resins as catalysts for aldose isomerization.

Resin	N Group	Matrix	A_{BET} [(1)] (m^2/g)	V_{pore} [(1)] (cm^3/g)	D_{pore} [(1)] (Å)	N [(2)] (wt%)	N [(2)] ($meq \cdot g^{-1}$)	Size [(3)] (μm)
IRA-67	tertiary amine	gel	<1.0	<0.01	-	2.10	1.5	500–750
A-21	tertiary amine	macroreticular	24.8	0.05	220	7.86	5.6	550
IRA-900	quaternary ammonium	macroreticular	7.5	0.10	80	4.62	3.3	640–800
A-26	quaternary ammonium	macroreticular	26.2	0.05	288	3.32	2.4	560–700

[(1)] Obtained from N_2 adsorption–desorption isotherms collected over dried samples of the resins; [(2)] Obtained by C, N, H elemental analysis; [(3)] Particle size as specified by the manufacturer.

Textural properties reflect that the members of the IRA family depict quite low porosity, with negligible pore volume and specific surface area values, as corresponding to gel-type resins after drying. Amberlyst materials, on the contrary, exhibited similar pore volumes and sizes and specific surface area values (24.8 and 26.2 m^2/g, respectively). Nevertheless, as indicated by the supplier, both types of materials, amberlyst and IRA resins, display a high swelling effect when in contact with water, being able to take up to 50 wt% of its own weight as water. Presumably, this conduct of the expansion of the porosity of the resin makes accessible the nitrogen basic sites by reactants when using aqueous phase reaction media [32–35].

Regarding the loading of catalytic basic sites, this is quite homogeneous, with little difference between the different resins. Basicity loadings between 1.5 and 5.6 meq·g^{-1} do not induce inferring any differences between the tested catalyst resins.

2.1. Isomerization of Glucose in the Presence of Different Anion Resins

2.1.1. Influence of the Temperature

The aqueous-phase isomerization of glucose to fructose was evaluated using the different Brønsted basic resins described above. The reaction was conducted under batch conditions, using 10 wt% glucose aqueous solutions as reaction media, and glucose/resin mass ratios of 1 for 120 min, varying the temperature conditions from 40 to 80 °C. Figure 1 shows the catalytic results obtained in the evaluation of the influence of the temperature conditions in the isomerization of glucose.

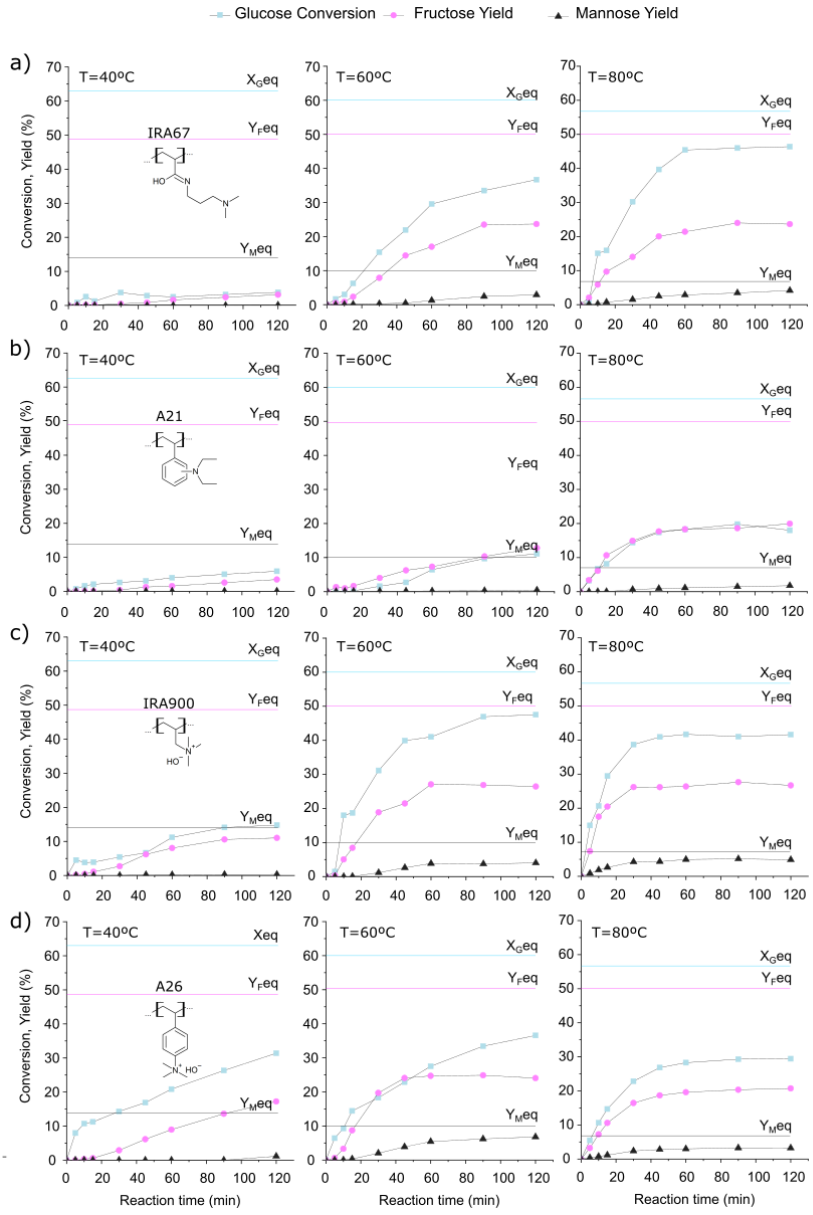

Figure 1. Isomerization of glucose into fructose in the presence of anion exchange resins at a constant substrate:resin mass ratio: (**a**) IRA-67, (**b**) A-21, (**c**) IRA-900 and (**d**) A-26. Reaction conditions of the initial substrate concentration: 10 wt% glucose in water; mass glucose/resin ratio = 1; temperature: 40–80 °C. Lines represent the equilibrium limits for substrate conversion (blue line), fructose yield (pink line) and mannose yield (black line).

As a general trend observed across all materials, the conversion of glucose and the yield to fructose increase with reaction temperature, although the fructose yield seems to be limited to 30%, so that higher product selectivity is achieved at the lower temperature conditions. Among the tested ion exchange resins, the members of the IRA family seemed to be more active than the Amberlyst materials—macroporous resins—probably because the higher basicity loading present in these materials, especially for IRA 900, favors a higher extension of the isomerization reaction. As for the influence of the strength of basic sites, resins bearing the stronger base sites of ammonium species conduct to higher fructose yields than weak resins portraying tertiary amine groups, regardless of the temperature conditions. Thus, IRA-67 and A-21 provided fructose yields no higher than 20%, whereas IRA-900 and A-26 exhibited a higher yield to fructose, 27% and 22% at 80 °C, respectively, which is consistent with previous reported studies on the activity of quaternary ammonium species [36]. All these values are far from the conversion limit imposed by thermodynamics calculated from equilibrium constants at the different temperatures, so that the limited production of fructose is not conditioned by the chemical equilibrium, but because of the existence of side reactions. Thus, in terms of product selectivity, IRA-900 revealed being superior to A-26 because of the very close values between substrate conversion and product yield, conducting to high selectivity values towards fructose (75%). The high extension of side reactions in the case of the A-26 resin causes a large mass deficit due to the generation of other products. One of those side products is mannose, which evolves from the isomerization of fructose under the tested reaction conditions. Other products, named degradation products, find their origin in the existence of side reactions involving the enolate intermediate produced during isomerization. Alternative pathways, such as the epimerization of glucose, is unlikely to be a feasible route, since this pathway requires harsher reaction conditions and, usually, the presence of strong Lewis acid catalysts [37–39]. Weak basic resins produced mannose in very low yields (below 3%), whereas IRA-900 and A-26 yielded up to 7% of the starting glucose as mannose at 80 °C. These results are quite close to those reported by Langlois and Larson, reaching a fructose yield of about 32% in the transformation of glucose assisted by highly basic anion exchange resins containing quaternary ammonium groups at similar temperature (87 °C) conditions [40].

The results obtained from the screening of basic anion resins as catalysts showed that the yield of fructose and the conversion of glucose in the isomerization reaction depend on the following factors: (1) the active sites determined by terminal functional groups: quaternary ammonium groups were found to exhibit greater fructose selectivity and glucose conversion compared to tertiary ammonium groups; and (2) the nature of the resin matrix: macroreticular porous resins provided a higher yield of fructose compared to gel-type resins. On the other hand, the thermal reaction conditions exhibited a net positive influence. Overall, IRA materials exhibited a very high dependence on the temperature conditions. Initially, at 40 °C, IRA resins provided poor glucose conversion with IRA-900 achieving a value of 15% and IRA-67 less than 10%. However, as the temperature increased to 60 °C, a significant improvement in glucose conversion was observed, achieving nearly 50% and 40% substrate conversion for IRA-900 and IRA-67, respectively, after 120 min, which is five times higher than that recorded at 40 °C. Additionally, the results achieved at 60 °C provide evidence that the initial reaction rate for IRA-900 resin was higher than that observed for IRA-67 resin. Apparently, this was due to the different textural properties of the two resins, as IRA-900 is a macroporous material that favors access to glucose, while the gel-type resin (IRA-67) offers lower porosity. Furthermore, by increasing the basicity of the catalyst, a higher isomerization rate is obtained. Finally, for IRA-900 (Figure 1c), a slight decrease in activity was observed when increasing the reaction temperature from 60 °C to 80 °C, which is close to the operation limit for this material. Changes in catalytic sites due to Hofman degradation of strong catalytic sites at 80 °C could be responsible for the decrease observed in the catalytic activity [41].

Proper optimization of the reaction conditions is crucial to achieve the desired conversion of glucose to fructose. In this sense, the strong basic resin IRA-900 demonstrates

promising catalytic performance under a mild reaction temperature of 60 °C, achieving a 41% glucose conversion and a 27% fructose yield at 60 min of reaction.

2.1.2. Kinetic Modeling

A comprehensive kinetic analysis was conducted on the isomerization of glucose to fructose in aqueous media. The analysis utilized experimental data obtained from various reaction temperatures and different basic anion exchange resins. This analysis allowed for the evaluation of a heterogeneous kinetic model and the assessment of the impact of experimental variables on the kinetic equation. The entire model was based on that proposed by Beenackers [42], and it was developed using a Python subrutine, fitting the experimental data to the proposed kinetic model by adjusting the values of the model parameters. A Langmuir–Hinshelwood–Hougen–Watson (LHHW) kinetic model was employed to reproduce the reaction rates included within Scheme 2.

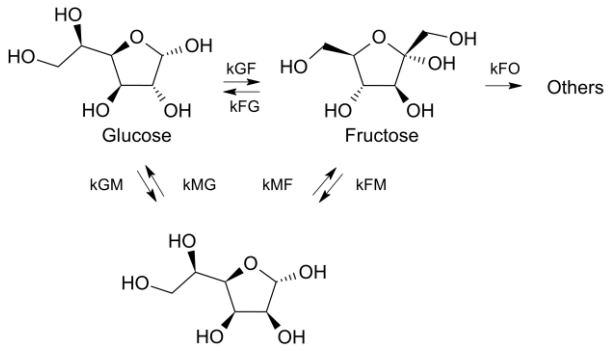

Scheme 2. Reaction network considered for kinetic modeling the isomerization of glucose in the presence of anion exchange resins.

This model considers the effects of adsorption, reaction, and desorption of the different chemicals involved within the reaction. The first pathway (G-F) illustrates the isomerization of glucose to fructose; the second pathway (F-M) involves the conversion of fructose to mannose; the third pathway (M-G) represents the conversion of mannose to glucose; and the fourth pathway (F-O) describes the degradation of fructose into other products.

Based on the proposed set of reactions included in Scheme 2 and based on the kinetic model developed by Beenackers [42], reaction rates can be described as follows:

$$r_{GF} = \frac{k_{GF} \cdot \left(C_G - \frac{1}{K_{eq-GF}} \cdot C_F \right)}{\frac{V_{sol}}{V_{pore}} + K_{AG} \cdot C_{OH_{ie}} + K_{AF} \cdot C_{OH_{ie}}} \quad (1)$$

$$r_{MF} = \frac{k_{FM} \cdot \left(C_F - \frac{1}{K_{eq-FM}} \cdot C_M \right)}{\frac{V_{sol}}{V_{pore}} + K_{AF} \cdot C_{OH_{ie}} + K_{AM} \cdot C_{OH_{ie}}}, \quad (2)$$

$$r_{GM} = \frac{k_{MF} \cdot \left(C_G - \frac{1}{K_{eq-GM}} \cdot C_M \right)}{\frac{V_{sol}}{V_{pore}} + K_{AG} \cdot C_{OH_{ie}} + K_{AM} \cdot C_{OH_{ie}}} \quad (3)$$

$$r_{OF} = \frac{k_{FDe} \cdot C_F}{\frac{V_{sol}}{V_{pore}} + K_{AF} \cdot C_{OH_{ie}}} \quad (4)$$

where, C_G, C_F, and C_M are the concentration of glucose, fructose and mannose, respectively; k_{GF}, k_{FM}, k_{GM}, and k_{GD} are the kinetic constants of the transformations glucose–fructose, fructose–glucose, fructose–mannose, mannose–fructose, glucose–mannose, mannose–glucose, and glucose–degradation products; K_{AG}, K_{AM}, and K_{AF} are the adsorption constants for glucose, mannose, fructose, and degradation products, respectively; V_{sol} and V_{pore} are the

volume of the solution outside the resin and total pore volume of the resin, respectively; and, finally, $C_{OH_{ie}}$.is the concentration of active sites in the resin. Adsorption and equilibrium constants were approached through van't Hoff-type equations as follows:

$$K_{eq} = K_{0eq} \cdot \exp\left(\frac{\Delta G}{RT}\right) \quad (5)$$

$$K_{ads} = K_{0ads} \cdot \exp\left(\frac{\Delta a}{RT}\right) \quad (6)$$

The equilibrium and adsorption constants were calculated from Equations (5) and (6) using the parameters provided by Beenackers for similar anion exchange resins to those used in our contribution. Values are given in Table 2.

Table 2. Equilibrium constants in isomerization reactions, and adsorption constants for glucose, fructose and mannose.

	Reaction/Component	K_0	ΔG (kJ·mol^{-1}·K^{-1})
Equilibrium	Glucose—Fructose	3.52×10^{-1}	3.48
	Fructose—Mannose	7.94×10^{-4}	15.37
	Glucose—Mannose	6.23×10^{-4}	18.44
Adsorption	Glucose	1.61×10^{-3}	10.01
	Fructose	5.49×10^{-3}	8.52
	Mannose	5.10×10^{-4}	13.36

Table 3 lists the obtained activation energies (Ea) of the different reactions proposed within the reaction network included in Scheme 2, for all the different tested resins. From the obtained results, it is evident that epimerization does not take place under the tested reaction conditions, bearing in mind the very high values achieved for the activation energy in this transformation. Recently, Delidovich [43] reported that the formation of mannose in the presence of bases occurs at a significantly slower rate compared to the formation of fructose, so that its production most likely occurs through the isomerization of glucose to fructose, and the subsequent isomerization of fructose to mannose. In addition to the formation of other products, the production of mannose is more prominent when utilizing the A-26 resin compared to IRA-900. The slower rate of mannose formation with the IRA-900 resin can be attributed to the significantly higher activation energy needed for the conversion of fructose to mannose (1.22×10^{10} J·kmol^{-1}·K^{-1} using IRA-900 compared to 1414.69 J·kmol^{-1}·K^{-1} for A-26). On the other hand, weak resins (IRA-67 and A-21) exhibited a higher activation energy for the conversion of route one (G-F) compared to strong resins (IRA-900 and A-26). This makes evident the requirement of stronger basic catalytic sites to obtain proper isomerization rates from glucose to fructose. However, the conversion to undesirable side products was more pronounced when employing the IRA-900 resin as a catalyst, providing a suitable explanation for the mass imbalance observed for this catalyst.

Table 3. Activation energies obtained from glucose isomerization for the different tested resins.

		IRA-67	A-21	IRA-900	A-26
Activation Energy (J·kmol^{-1}·K^{-1})	Ea_{GF}	78.33	58.31	77.61	30.94
	Ea_{FM}	2.30×10^{14}	140.80	1.22×10^{10}	1414.69
	Ea_{MG}	66.04	74.96	43.33	27.50
	Ea_{FO}	4.84×10^{-4}	1.08×10^{-4}	0.14	1.14×10^{-5}

Amberlyst IRA resins seemed to promote the transformation of glucose at similar rates, as ascertained by the similarity in activation energies obtained for the different considered transformations within Scheme 2. Notwithstanding, activation energy calculated for the isomerization of glucose to fructose was highly coincident in both IRA resins, so that the differences in terms of catalytic activity observed between both base catalysts should lay on the different strength of the catalytic sites. As for the amberlite resins, the fitting of kinetic data conducted to much lower activation energies when considering the isomerization of glucose. Nevertheless, the kinetic parameters evidenced the greater ease of the epimerization pathways for proceeding in the presence of these resins as compared to IRA materials. From these results, it seems evident that the tested members of the IRA families are more prone to promote the desired transformation, under the tested conditions, than amberlite materials. Moreover, among IRA resins, due to the stronger nature of the ammonium basic sites, IRA-900 seemed superior in terms of fructose, even though it also promotes side reactions in a higher extent.

Figure 2 provides the fitting of the proposed kinetic model to the experimental results (concentrations of glucose, fructose, and mannose) both as kinetic profiles (left) and as parity plots (right) for data collected for Amberlyst IRA 900 resin at different temperatures. A higher reaction rate is observed insofar as the temperature increases. However, after 2700 s of reaction time, the concentration of fructose reached at 60 °C exceeds that achieved at the 80 °C tests. At 7200 s, the fructose concentrations reached 167.78 mol/m^3 and 131.31 mol/m^3 for the 60 °C and 80 °C tests, respectively, suggesting that 60 °C were enough to maximize the production of fructose, whereas higher temperature conditions would lead to the production of higher amounts of side products, such as mannose or degradation products. Thus, the IRA-900 resin was specifically chosen because of its ability to maximize the yield of fructose while minimizing the formation of mannose at moderate temperature conditions.

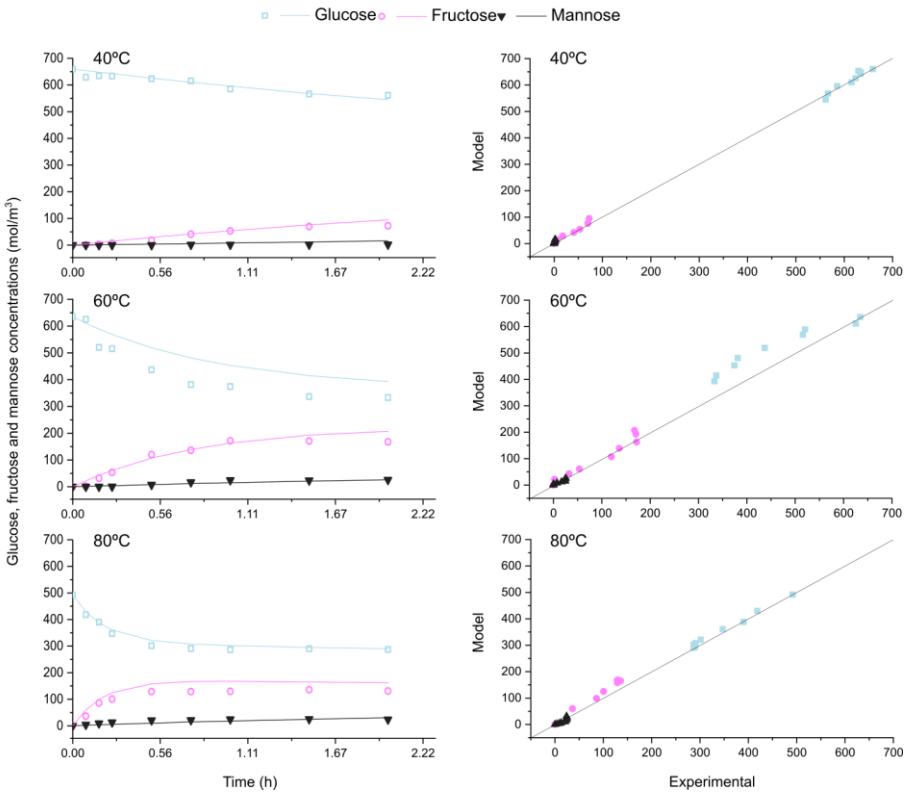

Figure 2. Experimental and calculated concentrations (**left**) and parity plots (**right**) obtained for glucose isomerization at different temperatures in the presence of IRA-900 resin. Data in mol·m^{-3}.

2.2. Isomerization of Hemicellulose Sugar Feedstock

To further investigate the catalytic performance and versatility of the selected IRA-900 resin in the isomerization of aldoses into ketoses, new tests were performed using different substrates. To this end, two sets of catalytic tests were carried out: (1) isomerization tests using different aldoses as substrates, including pentoses and hexoses; and (2) isomerization tests of complex sugar mixtures emulating different hemicelluloses.

2.2.1. Catalyst Versatility—Isomerization of C5 and C6 Aldoses

The catalytic performance of IRA-900 in the isomerization of aldopentoses and aldohexoses was evaluated under the reaction conditions previously established as the most adequate for glucose isomerization. Experiments were conducted with four sugars—xylose, arabinose, mannose, and galactose—allowing a straightforward comparison between C5 and C6 aldoses. The reaction conditions consisted of reaction temperature of 60 °C, a starting 10 wt% aqueous sugar solution, and a substrate/catalyst mass ratio of 1. Results from the isomerization tests are depicted in Figure 3.

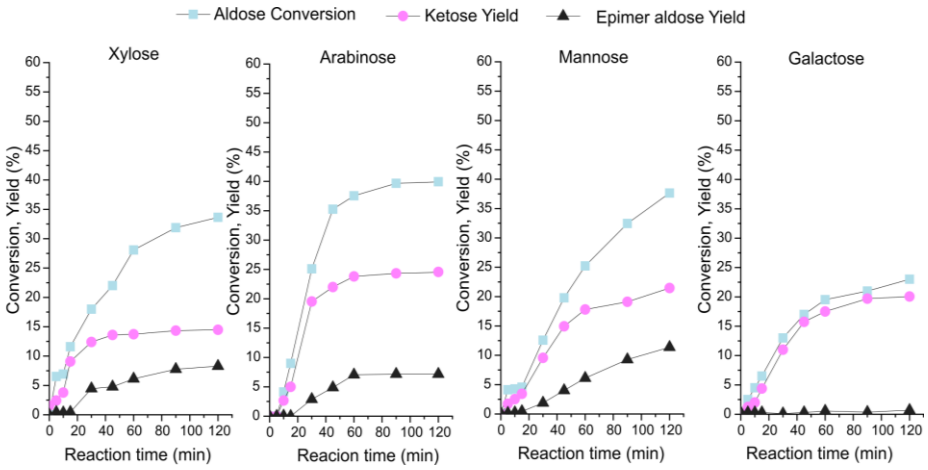

Figure 3. Isomerization of aldopentoses (xylose, arabinose) and aldohexoses (mannose, galactose) into their corresponding ketoses in the presence of IRA-900. Reaction conditions of the initial substrate concentration: 10 wt% sugar in water; mass sugar/resin ratio = 1; temperature: 60 °C.

The conversion of C5 aldoses into ketoses under basic conditions was described as proceeding faster than C6 sugars [44], which explains the higher initial reaction rate observed in the transformation of xylose and arabinose as compared to aldohexoses. Nevertheless, the reaction rate for the isomerization of sugar monosaccharides, is strongly dependent on the structure of the sugar. In this way, xylose and arabinose were transformed in a high extension, reaching conversion values of 29% and 38%, respectively, after 60 min, and slightly higher values at 120 min. Selectivity was quite high during the first stages of the reaction (70–80%) at 30 min, but afterwards, due to the high conversion values reached on the starting substrate, it abruptly dropped. Notably, in both cases, the formation of the epimer aldose (lyxose for xylose and ribose for arabinose), occurred in a high extension, providing quantifiable yields above 7% at the end of the catalytic runs. These two aldoses are not present in the reaction media during the first stages of the reaction runs, and they only appeared in the reaction media after the concentration of the corresponding ketose (xylulose and ribulose) reached high values. In this way, their formation seems to be linked to the isomerization of the ketose more than to the epimerization of the starting aldose, in a similar way to that described for glucose.

Regarding hexoses, mannose and galactose exhibited a lower reactivity as compared to glucose, reaching conversion values of 25% and 20%, respectively, after 60 min [45,46]. Upon increasing the reaction time up to 120 min, mannose reached a maximum conversion value of 40%, but at the expense of reducing the selectivity for the ketose, due to the

formation of huge amounts of glucose. On the other hand, galactose isomerization provided remarkable results, as a very high selectivity towards tagatose, the target product, was achieved. Interestingly no sorbose–tagatose epimer or talose–galactose epimer production was detected.

From these results, it is evident that the selected base resin IRA-900 is a versatile catalyst able to convert a multitude of aldoses (both pentoses and hexoses) into their corresponding ketoses; thus, an additional step in the evaluation of the capability of this resin was taken: the isomerization of mocking hemicellulose hydrolysate solutions.

2.2.2. Isomerization of Sugar Mixtures

Aiming to produce ketose-rich sugar streams from complex mixtures of monosaccharides, isomerization tests were conducted using different mixtures of pentoses and hexoses simulating different hemicellulose hydrolysates from several biomass feedstocks, including sugarcane bagasse—*Saccharum officinarum* L.—(SCB), white birch—*Betula papyfera*—(WB), eucalyptus (EU), and scots pine—*Pinus sylvestris*—(PS). Catalytic tests were performed using Amberlite IRA-900 basic anion resin as a solid catalyst at 60 °C for 2 h. Table 2 lists the concentration (g/L) of the different monosaccharides in the reaction media before and after the catalytic tests. Several monosaccharides have been omitted due to either low concentration values, or because the difficulty in the quantification of minor compounds in these highly complex mixtures.

The initial composition of the hemicellulose hydrolysates was assessed by directly characterizing hemicellulose fraction obtained through a GVL-based organosolv procedure [47]. The analysis of the monosaccharide composition evidenced important differences between the different raw materials, since SCB, WB, and EU hemicelluloses displayed quite a low concentration of C6 monosaccharides, whereas PS showed more evenly distributed concentrations between C5 (42.9%) and C6 (57.1%). By using all these feedstocks, it is possible to ascertain the versatility of the tested IRA-900 resin in the transformation of very different sugar-containing feedstock.

As previously observed in tests conducted for pure monosaccharides, C5 sugars—arabinose and xylose—were both converted to a high extent and faster than hexoses—mannose and galactose. On the other hand, the isomerization of these monosaccharides (regardless of whether a pentose or a hexose) was strongly dependent on the exact structure, being transformed at very different reaction rates. As for the case of the transformation of the different sugar mixtures, the observed trends for each single sugar seemed to be reproduced in the transformation of the different hemicellulose mock solutions (Table 4).

Table 4. Results of initial (Ci) and final (Cf) concentration distribution of each sugar (g/L) for different solutions emulating hemicellulose hydrolysates treated at 60 °C with IRA-900. Reaction conditions: initial sugar concentration = 100 g/L; sugar to resin mass ratio = 1; temperature conditions: 60 °C; reaction time: 120 min.

Monosaccharide		Sugarcane Bagasse		White Birch		Eucalyptus		Scots Pine	
		Ci (g/L)	Cf (g/L)	Ci (g/L)	Cf (g/L)	Ci (g/L)	Cf (g/L)	Ci (g/L)	Cf (g/L)
Hexoses	Mannose	0.2	0.0	2.7	1.9	3.4	1.9	46.5	29.4
	Galactose	3.0	1.5	9.7	7.7	9.7	7.8	9.1	7.5
	Glucose	-	0.1	-	1.6	-	0.5	-	6.9
	Fructose	-	0.1	-	0.9	-	0.9	-	9.6
	Tagatose	-	1.2	-	1.6	-	1.5	-	1.3
Pentoses	Xylose	85.4	58.3	85.7	49.7	83.0	59.8	33.9	16.6
	Arabinose	9.6	3.5	1.4	0.1	4.3	1.2	9.0	3.5
	Xylulose	-	13.3	-	13.1	-	12.7	-	4.8
	Ribulose	-	3.5	-	0.8	-	1.9	-	3.0
Total		98.2	81.5	99.5	76.6	100.4	88.3	98.5	82.6

Regarding raw materials SCB, WB, and EU, whose composition is quite similar, the catalytic conversion of xylose was consistently observed to occur at 30–40% across all cases, after the 2 h tests. Arabinose was converted in a higher extension than xylose, as it was previously observed in the transformation of single monosaccharides. The selectivity of the transformations of these two sugars towards the corresponding ketose was roughly 50% for xylose and above 60% for arabinose, which is in fairly good agreement with the values achieved for the tests conducted with single sugars. In the case of C6 sugars, mannose was converted to a moderate extension (30–40%), but much more than galactose, which exhibited an average conversion below 20% after the 2 h tests. As for the selectivity of the isomerization, while mannose transformation into fructose proceeded with an average selectivity of 50%, the transformation of galactose into tagatose occurred with a selectivity of 80%. Both values are similar to those expected bearing in mind the achieved results from the single sugar catalytic tests.

As for the transformation of mock PS hemicellulose solutions, results revealed no great differences in terms of sugar conversion and product yields, providing similar selectivities towards the different target ketoses included in Table 4. These results suggest the absence of crossed effects or interference between the transformation of the different sugars when other monosaccharides are present.

From the previous results, it can be concluded that the isomerization of the different tested sugar monosaccharides, both as single sugar solutions, and as a complex mixture mocking hemicellulose hydrolysates, can be accomplished in the presence of the basic resin IRA-900, providing suitable evidence of the high versatility of this catalyst. Nevertheless, there is one more question to address regarding the ability of this resin to function as heterogeneous catalyst in sugar isomerization reactions, which is its reusability.

2.3. Catalyst Reusability

Catalyst reusability was assessed by performing four consecutive reaction runs using the same catalyst sample, with intermediate washing in between consecutive reaction runs for glucose isomerization. Figure 4 show the results for IRA-900 in the reusability tests, and the analysis of the fresh and spent samples through FTIR and TG analyses.

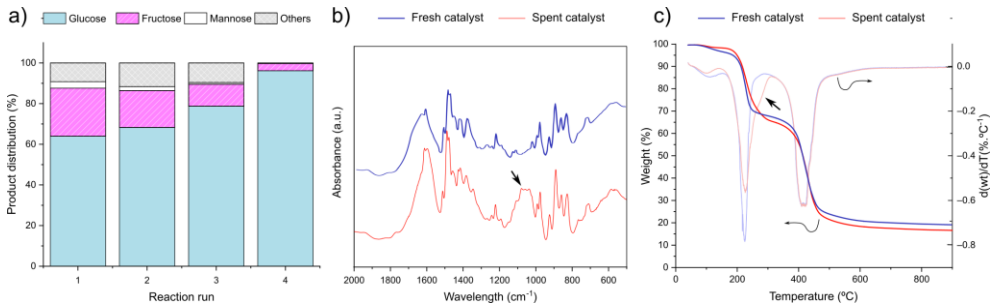

Figure 4. (**a**) Results from reusability tests of IRA-900 in the isomerization of glucose in water; (**b**) FTIR spectra recorded for fresh and spent catalyst samples; (**c**) thermogravimetric analysis of fresh and used catalyst sample. Reaction conditions of the initial substrate concentration: 10 wt% glucose; mass glucose/resin ratio = 1; temperature: 60 °C; reaction time: 60 min.

Reusability tests performed in water revealed a medium but progressive catalyst deactivation. The initial run provided almost 36% of glucose conversion, yielding 24% of fructose and 3% of mannose as the main products. Together with glucose isomers, unknown side products accounted for 9%. Nevertheless, the initial activity shown by the resin in the first reaction run, progressively diminished until a negligible conversion of the substrate (below 5%) was achieved in the fourth reaction run. Obviously, these results prompt to a catalyst deactivation, which progressively occurred with the different reaction cycles and was not prevented through the intermediate washing step.

To elucidate the cause of deactivation, samples of the spent catalyst were characterized through FTIR (Figure 4b) and thermogravimetric (Figure 4c) analyses. Depicted FTIR spectra correspond to the fresh and spent catalyst samples, and most of the detected signals can be attributed to functional groups in the organic matrix of the resins: the vibration band at 1630 cm^{-1} is attributed to the presence of adsorbed water; 1612 cm^{-1} signal correspond to N-H bending ascribed to the catalytic functional groups; and signals recorded at 977 and 897 cm^{-1} represent the deformation vibrations of 1,4-disubstituted benzene ring [48]. However, the most interesting differences between the spectra collected for the fresh and the spent anion resins were observed at 1772, 1100 and 1050 cm^{-1}. The signal at 1772 cm^{-1} is ascribed to chemical species bearing carboxylic groups, such as organic acids or lactones, indicating the formation of side products like sugar acids during the transformation of the starting monosaccharides. Nonetheless, this signal is low intense, meaning that the formation of such acid products occurs to a minor extension. On the other hand, signals at 1100 cm^{-1} and 1050 cm^{-1}—highlighted by an arrow in FTIR spectra—are attributed to the vibration of the C-O bond found in primary and secondary alcohols. The intensity of this signal is much higher, and the strong difference in this region between the spectra collected for the fresh and the spent catalyst sample indicate a significant modification. This observation could be attributed to the accumulation of sugars by entanglement within the porous matrix of the resin [49], so that a plausible reason for the deactivation could be the blocking of the catalytic sites during the reaction. Aiming to evaluate this possibility, thermogravimetric analysis was conducted for fresh and spent catalyst samples (Figure 4c). Both samples of the IRA-900 catalyst showed a large weight loss (~80%), as expected, because of the organic nature of the catalysts. The collected TGA curves show three steps in the decomposition with increasing temperature. The first thermal step, found in the range from 0 to 100 °C, is due to adsorbed water or organic solvents. The second step is associated with the degradation of nitrogen functional groups in the polymeric structure. This occurred at 224 °C and, despite a minimum weight loss difference observed between the fresh and spent catalyst samples, in the case of the spent catalysts, a double contribution to this weight loss was observed. This might be ascribed to the presence of organic deposits, formed by sugar molecules interacting with the nitrogen-base catalytic sites, most probably through ion exchange mechanisms. Final weight loss occurred at 425 °C, accounting for around 42% of the total weight, for both the fresh and the spent catalyst samples. This weight loss is ascribed to the degradation of the polymer matrix.

These results prompt to the deposition of organics inside the porous matrix of the resin as the main cause of deactivation, hindering the access of the substrate molecules to the catalytic basic sites. These organic deposits could be related to both the starting carbohydrate and to insoluble side products, such as cyclic lactones, or even sugar acids, having the potential to physically cover the surfaces of resin catalysts, thereby causing a reduction in catalytic activity.

The evaluation of the formation of organic deposits in spent catalyst samples after the reaction tests has been extended to those samples used in the isomerization of sugar mixtures emulating hemicellulose hydrolysates. Results are depicted in Figure 5.

Thermogravimetric analyses show the very same three weight loss stages found for samples used with glucose already described. The different thermogravimetric curves did not show significant differences but for the second decomposition stage. In this case, thermogravimetric curves exhibited the already described double contribution in all the four cases together with another contribution, but at a lower temperature. The extension of this new weight loss seems to be related to the presence of pentose sugars in the starting feedstock, as its contribution is lower in spent catalyst used with scots pine hemicellulose solutions than in any other sample of spent catalysts. In this way, the presence of C5 and C6 carbohydrate monosaccharides seems to lead to differences in the uptake of organic deposits, as the cause of catalyst deactivation in both cases is the adsorption of sugars onto the catalytic sites.

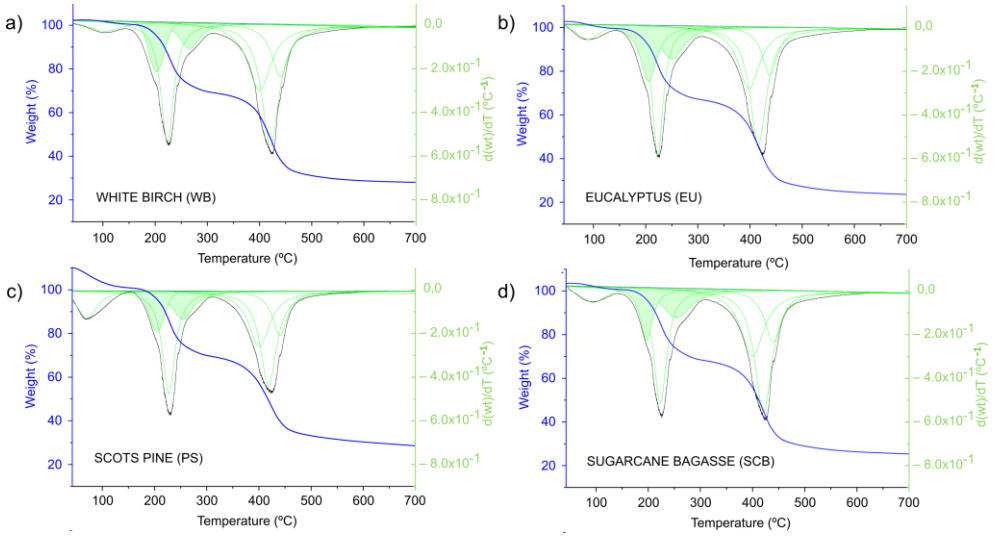

Figure 5. Results for thermogravimetric analysis of spent catalyst samples obtained from emulating sugar mixture isomerization reaction for different feedstocks with IRA-900: (**a**) WB; (**b**) EU; (**c**) PS and (**d**) SCB. Reaction conditions: mass substrate/catalyst ratio = 1, reaction temperature: 60 °C and reaction time: 60 min.

Aiming to reduce the deactivation of the porous basic resin IRA-900 in the isomerization of sugars, different organic solvents were used as cosolvents looking to favor the dissolution of organic side products causing the observed drop-in catalytic activity during the recycling tests performed in pure water. These solvents were selected among those showing a high swelling effect on IRA-90 [28], thus favoring mass transfer inside the porous catalyst particles and diminishing the risk of trapping organics because of entanglement with the polymer resin matrix. For this purpose acetonitrile (ACN), dimethylsulfoxide (DMSO), and ethanol were used as a cosolvent in a water:organic solvent weight ratio = 60:40.

Figure 6 displays the results of catalyst reuse obtained from the glucose isomerization reaction using IRA-900 with different reaction media. For aprotic polar solvents, they seemed to boost, in the first reaction run, the catalytic activity of the resin, providing a highly selective transformation of glucose toward fructose (30% yield) with minimum amounts of side products. Nevertheless, the production of fructose continuously dropped with every reusing test, whereas mass imbalance increased. DMSO-water mixtures registered the maximum value for glucose conversion at 44%, but with a lower selectivity for fructose, as compared to ACN. However, both the glucose conversion and the fructose yield dramatically decreased to almost a complete loss of activity at the fourth reusing cycle. Mun et al. [28] reported that high polar aprotic solvents conduct to low glucose conversion values in isomerization tests conducted in the presence of anion resins, probably because of the competition between the cosolvents and the sugar substrates for the adsorption to the porous resin. Nevertheless, the use of a high proportion of water in the reaction media used in our case might partially attenuate this effect.

Ethanol–water as reaction media seemed the most successful option to partially avoid catalyst deactivation, at least during the first reaction runs. Ethanol–water reaction media promoted the conversion of glucose, achieving 37% and 27% in the first and second reaction cycles, respectively, with fructose yields quite similar between them (25%). Nevertheless, together with fructose, higher production of mannose was also observed (7% yield), much higher than that obtained in water media. Additionally, mass imbalance was the lowest among the different tested solvents, supporting the idea that sugar degradation side reactions in aprotic solvents are more abundant compared to protic solvents [50].

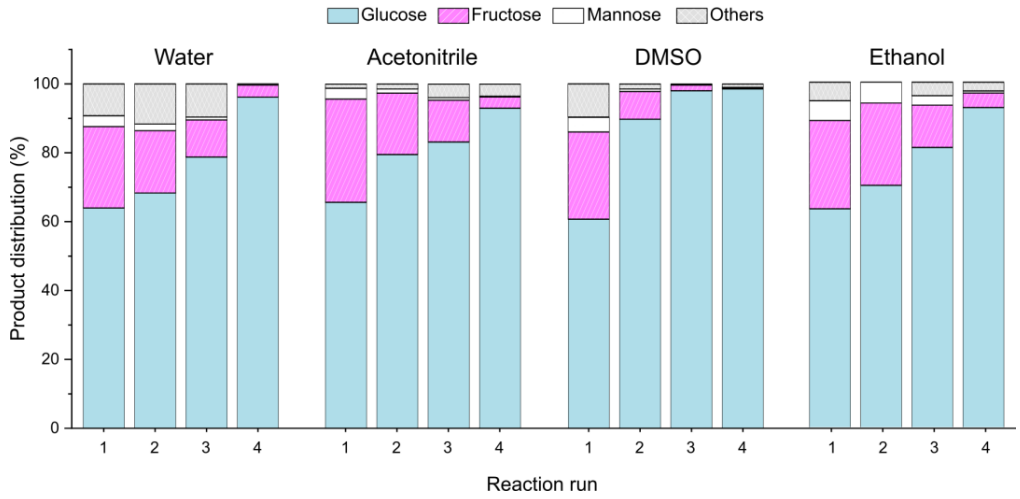

Figure 6. Results of catalyst reuse obtained from glucose isomerization reaction for different reaction medias with IRA-900. Reaction conditions: 10 wt% glucose; mass substrate/catalyst ratio = 1, reaction temperature: 60 °C and reaction time: 60 min.

Aiming to elucidate the effect of the presence of cosolvents in the enhanced reusability of IRA-900 resin, FTIR spectra collected for samples of IRA-900 used in water and ethanol–water as reaction media (Figure 7). The band located at 1100–1050 cm^{-1} attributed to the vibration of the C-O bond in primary and secondary alcohols, which is ascribed to the accumulation of sugars in the resin matrix, is the main difference between the collected spectra. Thus, whereas the signal is highly intense in the spent catalyst used in water media, that recorded for sample used in ethanol–water features a much lower intensity, suggesting that the accumulation of sugars is lower in the spent catalysts when ethanol is present in the reaction media.

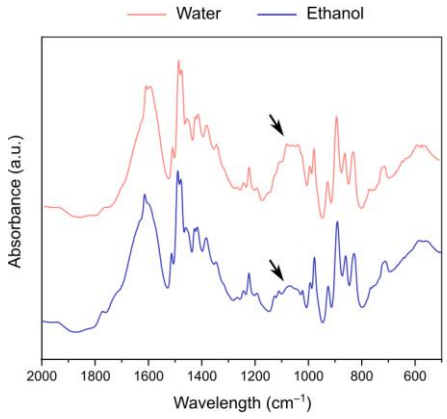

Figure 7. FTIR spectra recorded for spent samples of IRA-900 resin used in the isomerization of glucose in water (red line) and water-ethanol 60:40% (blue line) as reaction media.

The reasons for the beneficial effect of ethanol in the reusability of the IRA-900 resin might be several, like the enhancement of the porosity of the resin polymeric matrix, which favors mass transfer and could reduce the cumulation of entangled sugars—as it can be easily assessed in the lower intensity signal detected in the 1100–1000 cm^{-1} region, highlighted with arrows—, or the competition between ethanol and the sugar substrates for adsorption onto the catalytic sites, which (partially) reduces the retention of the monosaccharides or even a combination of the same. However, it seems evident that the use of ethanol exerts a positive effect in catalyst recyclability; however, deeper insights into the exact nature of this effect might require extended experimental activity.

Finally, the strategy of using ethanol as a reaction cosolvent for enhancing the reusability of the IRA-900 resin was extended to sugar mixtures mocking scots pine hemicellulose hydrolysates. This mixture was selected over the rest of the hemicellulose mocking solutions because it shows a more complex composition, with similar contents of hexoses and pentoses. Table 5 presents the initial and final concentration distribution of each sugar monosaccharide.

Table 5. Results of reusability in ethanol–water mixtures (40/60 vol). Initial and final concentration distribution of sugar monosaccharides (g/L) in emulated scots pine hemicellulose treated at 60 °C with IRA-900.

Monosaccharide		Sugar Concentration (g/L)				
		Initial	Reuse 1	Reuse 2	Reuse 3	Reuse 4
Hexoses	Mannose	44.6	31.6	32.3	36.9	38.3
	Galactose	10.6	7.4	8.3	9.6	9.7
	Glucose	-	2.0	1.6	0.0	0.0
	Fructose	-	8.5	7.6	2.0	1.6
	Tagatose	-	2.7	1.9	0.0	0.0
Pentoses	Xylose	39.4	26.2	27.9	26.5	31.3
	Arabinose	10.9	7.6	8.5	9.5	9.7
	Xylulose	-	11.0	8.8	7.8	3.9
	Ribulose	-	2.7	1.7	0.0	0.0
Total		105.5	99.5	98.1	92.3	94.5

Conversion of all the monosaccharides was well kept during the first and second reaction runs but dropped to minimum values in the fourth cycle. This was a general trend except for xylose, whose conversion remained constant during all the reaction runs (ca. 30%). Nevertheless, ketose yields experienced a constant and progressive reduction, indicating that the effect of ethanol was similar to all of them—hexoses and pentoses—and thus, the strategy seems to be applicable to different sugar feedstocks, regardless of their composition.

3. Experimental

3.1. Materials and Methods

Amberlite IRA-900 (SUPELCO, Madrid, Spain), Amberlyst A-26 (SUPELCO, Madrid, Spain), Amberlite IRA-67 (Alfa Aesar, Lancashire, UK), and Amberlyst A-21 (Alfa Aesar) basic resins were tested as catalysts in isomerization reactions. All the resins were conditioned to remove possible physisorbed impurities on the catalyst surface [23], using diluted NaOH aqueous solutions. The activation procedure comprised washing the resins with ultrapure water in a Soxhlet apparatus overnight, contacting them with 1 mol/L NaOH solution and a final washing step with ultrapure water in a Soxhlet apparatus under N_2 atmosphere overnight. Active resins were stored under inert atmosphere prior to their use in catalytic tests [36,49].

Glucose (99.5%, Sigma-Aldrich, Darmstadt, Germany), arabinose (98%, Sigma-Aldrich), mannose (99%, Alfa Aesar), galactose (99%, TCI, Tokyo, Japan), and xylose (99%, Acros Organics, New Jersey, EE. UU.) were used as reactants without previous purification, and as chromatography standards for HPLC calibrations. Dimethyl sulfoxide (99%, Scharlab, Barcelona, Spain), acetonitrile (99%, Scharlab), and ethanol (98%, Scharlab), were used as cosolvents in reusability tests as received.

3.2. Catalyst Characterization

Textural properties were determined from N_2 physisorption isotherms recorded at 77 K using a Micromeritics Tristar 3000 equipment. Samples were outgassed at 100 °C prior to their analysis. The specific surface area was calculated by the B.E.T. method (S_{BET}), average pore size was calculated using the B.J.H. method, and the total pore volume (Vp)

was assumed to be that recorded at p/p_0 = 0.95 [51]. CHNS elemental analyses were obtained using a Thermo Scientific Flash 2000 CHNS-O equipment. Fourier transform infrared spectroscopy (FTIR) analyses were performed on FT-IR Frontier (PELKIN ELMER) equipment. Spectra were collected in the range 4000–400 cm^{-1} at room temperature using the KBr buffer technique. Typically, samples were mixed with KBr (1 wt%) and mechanically compressed to form a 1 cm diameter tablet.

3.3. Catalytic Activity

Catalytic activity tests were performed in a round-bottom flask fitted with a magnetic stirrer and using water, or water-cosolvents, as reaction media. Typically, 10 wt% aqueous solution of an aldose monosaccharide, or a mixture of monosaccharides, was treated with the basic resins, using a mass ratio substrate/resin = 1. Temperature conditions were explored in the range 40–80 °C. Sample aliquots were periodically withdrawn from the reaction media at 5, 10, 15, 30, 45, 60 and 120 min. Reaction products were analyzed by HPLC using Aminex HPX-87P (Biorad) and HiPlex-H (Agilent Technologies) columns for product separation. Typical analysis conditions were the following: for Aminex HPX-87P, column temperature at 80 °C and 0.5 mL H_2O/min as mobile phase; and for HiPlex-H, column temperature at 60 °C and 0.6 mL of 0.005M H_2SO_4/min as mobile phase. Detection was performed using a refraction index detector. Calibration curves for each single sugar were calculated separately using standard stock solutions of carbohydrates, with known concentration. Catalytic results were calculated as follows:

$$X_S(\%) = \frac{Converted\ moles\ of\ substrate}{Initial\ moles\ of\ substrate} \cdot 100 \quad (7)$$

$$Y_i(\%) = \frac{Moles\ of\ product\ generated}{Inital\ moles\ of\ substrate} \cdot 100 \quad (8)$$

$$S_i(\%) = \frac{Y_i}{X_s} \cdot 100 \quad (9)$$

where X_S is the conversion of the substrate, $Y_i(\%)$ is the yield of product i (fructose or mannose), and $S_i(\%)$ is the selectivity towards each product.

3.4. Catalyst Reusability

The reusability of IRA-900 was evaluated through recycling tests, recovering the catalysts by filtration after the reaction, washing it, and using it again in a new test, for four consecutive reaction cycles. In the case of catalyst reusability tests performed in the presence of different organic solvents, these were tested as reaction media, aiming to reduce organic deposition. Dimethyl sulfoxide (DMSO), acetonitrile (ACN) and ethanol were selected as cosolvents to prepare 60/40 vol water/organic solvent mixtures to be used as reaction media. All these solvents showed complete miscibility and high-solvency capacity to dissolve 10 wt% of glucose. Spent catalysts were treated by washing with fresh mixtures of the reaction media in between different recycling runs. The washing treatment involved stirring the resin for 10 min at room temperature using a magnetic stirrer to clean the resin and recover active basic centers.

4. Conclusions

Mild reaction conditions are required to obtain proper glucose conversion and fructose yields (ca. 20–27% at 1 h) using Brønsted base anion exchange resins as catalysts. Among the different tested materials, IRA-900 resin displays superior performance over the rest of the tested resins because of a combination of strong basic sites with a porous structure. This material is a highly versatile catalyst able to convert other substrates, including hexoses (mannose and galactose), and pentoses (xylose and arabinose), with similar yields to glucose, although the extension of the transformation strongly depended on the substrate

structure. Additionally, synthetic mixtures emulating hemicellulose hydrolysates, bearing aldohexoses and aldopentoses, were equally converted into the corresponding ketoses, with a similar catalytic performance to that shown for single sugars. Nevertheless, the IRA-900 resin suffered a strong deactivation, due to the cumulation of sugars inside the porous structure of the material. The addition of ethanol to the reaction medium improved the catalyst reusability by partially preventing the retention of sugars in the spent catalysts. Despite the stability of the system remains unresolved, because the deactivation is progressive with each reaction cycle, the use of ethanol, or analogue protic solvents, as cosolvent for sugar isomerization, it appears as an interesting pathway to explore in the isomerization of sugar aldoses into their corresponding ketoses. Deeper insights in the beneficial effect of the use of cosolvents and the possibility of regenerating the anion exchange resins will then have to be resolved. Finally, the evaluation of the transformation of complex mixtures of sugars, such as those produced from hemicellulose hydrolysates like the work here described, has been scarcely reported, although it is a highly interesting pathway to include alternative biomass-derived feedstock in the promotion of a chemical industry based on renewable raw materials.

Author Contributions: M.E.T.-L.: Investigation, data curation, Formal analysis; M.M.: Investigation, Validation, data curation, Formal analysis, Conceptualization, Methodology, Writing—original draft preparation. M.M.-V.: Investigation, J.M.: Conceptualization, Methodology, Writing—review and editing, Supervision, Project administration, Funding acquisition. J.I.: Conceptualization, Methodology, Writing—review and editing, Visualization, Project administration, Funding acquisition. All authors have read and agreed to the published version of the manuscript.

Funding: This research was funded by the Spanish Ministry of Science and Innovation (project PID2021-122736OB-C44). This research was funded by Bio Based Industries Joint Undertaking (JU) under the European Union's Horizon 2020 research and innovation program under grant agreement No 101023202.

Data Availability Statement: The data presented in this study are available on request from the corresponding author.

Acknowledgments: This research was funded by the Spanish Ministry of Science and Innovation (project PID2021-122736OB-C44). This work has received funding from the Bio-based Industries Joint Undertaking (JU) under the European Union's Horizon 2020 research and innovation program under grant agreement 101023202. The JU receives support from the European Union's Horizon 2020 research and innovation program and the Bio-based Industries Consortium. David Martin-Alonso is kindly acknowledged for providing compositions of hemicellulose hydrolysates.

Conflicts of Interest: The authors declare no conflict of interest.

References

1. Tayyab, M.; Noman, A.; Islam, W.; Waheed, S.; Arafat, Y.; Ali, F.; Zaynab, M.; Lin, S.; Zhang, H.; Lin, W. Bioethanol Production from Lignocellulosic Biomass by Environment-Friendly Pretreatment Methods: A Review. *Appl. Ecol. Environ. Res.* **2018**, *16*, 225–249. [CrossRef]
2. Ashokkumar, V.; Venkatkarthick, R.; Jayashree, S.; Chuetor, S.; Dharmaraj, S.; Kumar, G.; Chen, W.H.; Ngamcharussrivichai, C. Recent Advances in Lignocellulosic Biomass for Biofuels and Value-Added Bioproducts—A Critical Review. *Bioresour. Technol.* **2022**, *344*, 126195. [CrossRef] [PubMed]
3. Haq, I.U.; Qaisar, K.; Nawaz, A.; Akram, F.; Mukhtar, H.; Zohu, X.; Xu, Y.; Mumtaz, M.W.; Rashid, U.; Ghani, W.A.W.A.K.; et al. Advances in Valorization of Lignocellulosic Biomass towards Energy Generation. *Catalysts* **2021**, *11*, 309. [CrossRef]
4. Velvizhi, G.; Goswami, C.; Shetti, N.P.; Ahmad, E.; Kishore Pant, K.; Aminabhavi, T.M. Valorisation of Lignocellulosic Biomass to Value-Added Products: Paving the Pathway towards Low-Carbon Footprint. *Fuel* **2022**, *313*, 122678. [CrossRef]
5. Singhvi, M.S.; Gokhale, D.V. Lignocellulosic Biomass: Hurdles and Challenges in Its Valorization. *Appl. Microbiol. Biotechnol.* **2019**, *103*, 9305–9320. [CrossRef] [PubMed]
6. Ji, X.J.; Huang, H.; Nie, Z.K.; Qu, L.; Xu, Q.; Tsao, G.T. Fuels and Chemicals from Hemicellulose Sugars. *Adv. Biochem. Eng. Biotechnol.* **2012**, *128*, 199–224. [CrossRef] [PubMed]
7. Hoydonckx, H.E.; Van Rhijn, W.M.; Van Rhijn, W.; De Vos, D.E.; Jacobs, P.A. Furfural and Derivatives. In *Ullmann's Encyclopedia of Industrial Chemistry*; Wiley: Weinheim, Germany, 2007. [CrossRef]

8. Li, H.; Yang, S.; Saravanamurugan, S.; Riisager, A. Glucose Isomerization by Enzymes and Chemo-Catalysts: Status and Current Advances. *ACS Catal.* **2017**, *7*, 3010–3029. [CrossRef]
9. Demerdash, M.; Attia, R.M. Equilibrium Kinetics of D-Glucose to D-Fructose Isomerization Catalyzed by Glucose Isomerase Enzyme from Streptomyces Phaeochromogenus. *Zentralbl. Mikrobiol.* **1992**, *147*, 297–303. [CrossRef]
10. Takasaki, Y. Kinetic and Equilibrium Studies on D-Mannose-d-Fructose Isomerization Catalyzed by Mannose Isomerase from Streptomyces Aerocolorigenes. *Agric. Biol. Chem.* **1967**, *31*, 435–440. [CrossRef]
11. Spencer, K.C.; Boisrobert, C.E.; Fisher, S.A.; Rojak, P.A.; Sabatini, K.S. Method of Producing High Fructose Corn Syrup from Glucose Using Noble Gases. U.S. Patent US5512464A, 25 December 1992.
12. Paniagua, M.; Saravanamurugan, S.; Melian-Rodriguez, M.; Melero, J.A.; Riisager, A. Xylose Isomerization with Zeolites in a Two-Step Alcohol-Water Process. *ChemSusChem* **2015**, *8*, 1088–1094. [CrossRef]
13. Drabo, P.; Delidovich, I. Catalytic Isomerization of Galactose into Tagatose in the Presence of Bases and Lewis Acids. *Catal. Commun.* **2018**, *107*, 24–28. [CrossRef]
14. Choudhary, V.; Pinar, A.B.; Sandler, S.I.; Vlachos, D.G.; Lobo, R.F. Xylose Isomerization to Xylulose and Its Dehydration to Furfural in Aqueous Media. *ACS Catal.* **2011**, *1*, 1724–1728. [CrossRef]
15. Delidovich, I.; Palkovits, R. Catalytic Isomerization of Biomass-Derived Aldoses: A Review. *ChemSusChem* **2016**, *9*, 547–561. [CrossRef] [PubMed]
16. Moliner, M.; Román-Leshkov, Y.; Davis, M.E. Tin-Containing Zeolites Are Highly Active Catalysts for the Isomerization of Glucose in Water. *Proc. Natl. Acad. Sci. USA* **2010**, *107*, 6164–6168. [CrossRef] [PubMed]
17. Román-Leshkov, Y.; Moliner, M.; Labinger, J.A.; Davis, M.E. Mechanism of Glucose Isomerization Using a Solid Lewis Acid Catalyst in Water. *Angew. Chem. Int. Ed.* **2010**, *49*, 8954–8957. [CrossRef] [PubMed]
18. Delidovich, I. Recent Progress in Base-Catalyzed Isomerization of D-Glucose into D-Fructose. *Curr. Opin. Green Sustain. Chem.* **2021**, *27*, 100414. [CrossRef]
19. Wolfromwi, M.L.; Lee Lewis, W. The Reactivity of the Methylated Sugars. II. The Action of Dilute Alkali on Tetramethyl Glucose. *J. Am. Chem. Soc.* **1928**, *50*, 837–854. [CrossRef]
20. Carraher, J.M.; Fleitman, C.N.; Tessonnier, J.P. Kinetic and Mechanistic Study of Glucose Isomerization Using Homogeneous Organic Brønsted Base Catalysts in Water. *ACS Catal.* **2015**, *5*, 3162–3173. [CrossRef]
21. Lobry De Bruyn, C.A. Action Des Alcalis DiIués Sur Ies Hydrates de Carbone I. *Recl. Des Trav. Chim. Des Pays-Bas* **1895**, *14*, 156–165. [CrossRef]
22. Saravanamurugan, S.; Paniagua, M.; Melero, J.A.; Riisager, A. Efficient Isomerization of Glucose to Fructose over Zeolites in Consecutive Reactions in Alcohol and Aqueous Media. *J. Am. Chem. Soc.* **2013**, *135*, 5246–5249. [CrossRef]
23. Bermejo-Deval, R.; Gounder, R.; Davis, M.E. Framework and Extraframework Tin Sites in Zeolite Beta React Glucose Differently. *ACS Catal.* **2012**, *2*, 2705–2713. [CrossRef]
24. de Bruijn, J.M.; Kieboom, A.P.G.; van Bekkum, H. Alkaline Degradation of Monosaccharides V: Kinetics of the Alkaline Isomerization and Degradation of Monosaccharides. *Recl. Des Trav. Chim. Des Pays-Bas* **1987**, *106*, 35–43. [CrossRef]
25. Mendicino, J.F. Effect of Borate on the Alkali-Catalyzed Isomerization of Sugars. *J. Am. Chem. Soc.* **1960**, *82*, 4975–4979. [CrossRef]
26. Shaw, A.; Tsao, G.T. Isomerization of D-Glucose with Sodium Aluminate: Kinetics as a Function of Temperature. *Carbohydr. Res* **1978**, *60*, 376–382. [CrossRef]
27. Ventura, M.; Mazarío, J.; Domine, M.E. Isomerization of Glucose-to-Fructose in Water over a Continuous Flow Reactor Using Ca−Al Mixed Oxide as Heterogeneous Catalyst. *ChemCatChem* **2022**, *14*, e202101229. [CrossRef]
28. Mun, D.; Huynh, N.T.T.; Shin, S.; Kim, Y.J.; Kim, S.; Shul, Y.G.; Cho, J.K. Facile Isomerization of Glucose into Fructose Using Anion-Exchange Resins in Organic Solvents and Application to Direct Conversion of Glucose into Furan Compounds. *Res. Chem. Intermed.* **2017**, *43*, 5495–5506. [CrossRef]
29. Lv, L.; Guo, X.; Bai, P.; Zhao, S. Isomerization of Glucose into Fructose and Mannose in Presence of Anion-Exchanged Resins. *Asian J. Chem.* **2015**, *27*, 2774–2778. [CrossRef]
30. Mäki-Arvela, P.; Salmi, T.; Holmbom, B.; Willför, S.; Murzin, D.Y. Synthesis of Sugars by Hydrolysis of Hemicelluloses- A Review. *Chem. Rev.* **2011**, *111*, 5638–5666. [CrossRef]
31. Zhang, X.; Wilson, K.; Lee, A.F. Heterogeneously Catalyzed Hydrothermal Processing of C5-C6 Sugars. *Chem. Rev.* **2016**, *116*, 12328–12368. [CrossRef]
32. Schouten, N.; van der Ham, L.G.J.; Euverink, G.J.W.; de Haan, A.B. Selection and Evaluation of Adsorbents for the Removal of Anionic Surfactants from Laundry Rinsing Water. *Water Res.* **2007**, *41*, 4233–4241. [CrossRef]
33. Souzanchi, S.; Nazari, L.; Rao, K.T.V.; Yuan, Z.; Tan, Z.; Xu, C. Catalytic Isomerization of Glucose to Fructose Using Heterogeneous Solid Base Catalysts in a Continuous-Flow Tubular Reactor: Catalyst Screening Study. *Catal. Today* **2019**, *319*, 76–83. [CrossRef]
34. Berbar, Y.; Amara, M.; Kerdjoudj, H. Anion Exchange Resin Applied to a Separation between Nitrate and Chloride Ions in the Presence of Aqueous Soluble Polyelectrolyte. *Desalination* **2008**, *223*, 238–242. [CrossRef]
35. Inczedy, J. Thermoanalytical Investigation of Ion Exchange Resins. The Swelling Water of Anion Exchange Resins. *J. Therm. Anal.* **1978**, *13*, 257–261. [CrossRef]
36. Beenackers, J.A.W.M.; Kuster, B.F.M.; Van Der Barn, H.S. Physical Properties of Anion Exchangers Used as a Catalyst in the Isomerization of Hexoses. *Appl. Catal.* **1985**, *16*, 75–87. [CrossRef]

37. Bermejo-Deval, R.; Orazov, M.; Gounder, R.; Hwang, S.J.; Davis, M.E. Active Sites in Sn-Beta for Glucose Isomerization to Fructose and Epimerization to Mannose. *ACS Catal.* **2014**, *4*, 2288–2297. [CrossRef]
38. Nguyen, H.; Nikolakis, V.; Vlachos, D.G. Mechanistic Insights into Lewis Acid Metal Salt-Catalyzed Glucose Chemistry in Aqueous Solution. *ACS Catal.* **2016**, *6*, 1497–1504. [CrossRef]
39. Chethana, B.K.; Mushrif, S.H. Brønsted and Lewis Acid Sites of Sn-Beta Zeolite, in Combination with the Borate Salt, Catalyze the Epimerization of Glucose: A Density Functional Theory Study. *J. Catal.* **2015**, *323*, 158–164. [CrossRef]
40. Langlois, D.P.; Larson, R.F. Interconversion of Sugars Using Anion Exchange Resins. U.S. Patent US2746889A, 22 May 1955.
41. Tianshu, B.; Lixuan, Z.; Chunhong, W. The Synthesis of Thermostable, Strongly Basic Anion-Exchange Resins Using Cross-Linked Biguanide and Its Application in the Extraction of Sodium Copper Chlorophyllin. *J. Chromatogr. B Anal. Technol. Biomed. Life Sci.* **2022**, *1211*, 123436. [CrossRef]
42. Beenackers, J.A.W.M. The Kinetics of the Heterogeneous Alkaline Isomerization of Carbohydrates. Doctoral Thesis, Technische Hogeschool Eindhoven, Eindhoven, The Netherlands, 1980. [CrossRef]
43. Delidovich, I. Toward Understanding Base-Catalyzed Isomerization of Saccharides. *ACS Catal.* **2023**, *13*, 2250–2267. [CrossRef]
44. Wang, W.; Mittal, A.; Pilath, H.; Chen, X.; Tucker, M.P.; Johnson, D.K. Simultaneous Upgrading of Biomass-Derived Sugars to HMF/Furfural via Enzymatically Isomerized Ketose Intermediates. *Biotechnol. Biofuels* **2019**, *12*, 253. [CrossRef]
45. Murzin, D.Y.; Murzina, E.V.; Aho, A.; Kazakova, M.A.; Selyutin, A.G.; Kubicka, D.; Kuznetsov, V.L.; Simakova, I.L. Aldose to Ketose Interconversion: Galactose and Arabinose Isomerization over Heterogeneous Catalysts. *Catal. Sci. Technol.* **2017**, *7*, 5321–5331. [CrossRef]
46. Milasing, N.; Khuwijitjaru, P.; Adachi, S. Isomerization of Galactose to Tagatose Using Arginine as a Green Catalyst. *Food Chem.* **2023**, *398*, 133858. [CrossRef] [PubMed]
47. Alonso, D.M.; Hakim, S.H.; Zhou, S.; Won, W.; Hosseinaei, O.; Tao, J.; Garcia-Negron, V.; Motagamwala, A.H.; Mellmer, M.A.; Huang, K.; et al. Increasing the Revenue from Lignocellulosic Biomass: Maximizing Feedstock Utilization. *Sci. Adv.* **2017**, *3*, 1603301. [CrossRef] [PubMed]
48. Wawrzkiewicz, M.; Hubicki, Z. Removal of Tartrazine from Aqueous Solutions by Strongly Basic Polystyrene Anion Exchange Resins. *J. Hazard. Mater.* **2009**, *164*, 502–509. [CrossRef] [PubMed]
49. Abu, A.; Abdullah, N. Sorption and Thermodynamic Study of Nitrate Removal by Using Amberlite IRA 900 (AI900) Resin. *Mater. Today Proc.* **2020**, *41*, 102–108. [CrossRef]
50. Drabo, P.; Fischer, M.; Emondts, M.; Hamm, J.; Engelke, M.; Simonis, M.; Qi, L.; Scott, S.L.; Palkovits, R.; Delidovich, I. Solvent Effects on Catalytic Activity and Selectivity in Amine-Catalyzed D-Fructose Isomerization. *J. Catal.* **2023**, *418*, 13–21. [CrossRef]
51. Thommes, M.; Kaneko, K.; Neimark, A.V.; Olivier, J.P.; Rodriguez-Reinoso, F.; Rouquerol, J.; Sing, K.S.W. Physisorption of Gases, with Special Reference to the Evaluation of Surface Area and Pore Size Distribution (IUPAC Technical Report). *Pure Appl. Chem.* **2015**, *87*, 1051–1069. [CrossRef]